International Journal of Mass Spectrometry 284 (2009) 81–92

Contents lists available at ScienceDirect

International Journal of Mass Spectrometry

journal homepage: www.elsevier.com/locate/ijms

Ageing behaviour and analytical characterization of the *Jatobá* resin collected from *Hymenaea stigonocarpa* Mart.

María Teresa Doménech-Carbó[a,*], Juana de la Cruz-Cañizares[a], Laura Osete-Cortina[a], Antonio Doménech-Carbó[b], Helena David[a,c]

[a] *Institut de Restauració del Patrimoni, Universitat Politécnica de València, Camino de Vera 14, 46022 Valencia, Spain*
[b] *Departament de Química Analítica, Universitat de València, Avda. Dr. Moliner s/n, 46100 Burjassot, Spain*
[c] *CAPES. Ministerio de Educaçao, Brazil*

ARTICLE INFO

Article history:
Received 27 February 2008
Received in revised form 17 December 2008
Accepted 22 December 2008
Available online 31 December 2008

Keywords:
GC–MS
Py–GC–MS
Varnish
Jatobá resin
Hymenaea stigonocarpa Mart.

ABSTRACT

This paper reports the results of an analytical study to characterize the trunk resin collected from the *Hymenaea stigonocarpa* Mart. species from the region of Minas Gerais (Brazil), popularly known as *Jatobá* resin. Hymenaea resins are reported to have been used in artistic applications such as protective varnishes in polychromed sculptures and paintings. Therefore, the identification of the main chemical changes that take place in the resin when it is prepared as a thin film exposed to atmospheric effects have been considered herein. Changes due to the degradation effect of light have been studied on a series of specimens prepared as a thin films and subjected to accelerated UV light ageing. The results based on GC–MS, THM–Py–GC–MS analyses, and on-line trimethylsilylation Py–GC–MS using hexamethyldislylazane as a derivatization reagent, have been compared. The study shows that eperuic acid and its Δ7 and Δ8 isomers, together with copalic acid, are the major components of the studied resin. Other compounds such as kolavenic acid, iso-ozic acid and *epi*-pinifolic acid are also present in this resin as minor components. This composition differs from those of resins obtained from other species of the *Hymenaea* genus growing in this Amazonian region. UV light ageing of the *Jatobá* resin prepared as a thin film results in the appearance of a new isomer of eperuic acid. Some changes in the relative content of the major components present in the resin have also been observed after ageing.

1. Introduction

Among the plants yielding diterpenoid resins, seventeen species of the neotropical leguminous genus *Hymenaea* (*Caesalpinoideae*, Detarieae, Cynometreae) [1], are largely distributed from Central to South America, mainly in the Amazon basin [2–5]. The resinous products of *Hymenaea* occur as opaque (sometimes translucent) fragments of a pale-yellow or nearly white colour. These products are commonly given the Brazilian name "jutaisica (or jutahyica) resin (from the term "yataiwa" of the Tupi language, meaning tree of hard fruit), elsewhere known as "Brazil Copal", "Brazil Dammar" or *Jatobá* resin (Fig. 1). From an analytical point of view, a number of published research can be found in the phytochemical literature dealing with the characterization of the composition of the *Hymenaea* resins [1–12]. As a result of these studies, *Hymenaea* species are known to mainly contain the diterpenoid compounds of an *epi*-labdanoid type in the trunk resin and bark extract. The *epi*-labdanoid series is the parallel *epimer* series in which the stereochemistry of the chiral centres at positions C(9) or C(10) (Fig. 2) is inverted. Interestingly, no papers have been found concerning resins of the species *Hymenaea stigonocarpa* Mart., which grows profusely in the Peruaçu valley (Minas Gerais, Brazil) and which this paper aims to study (*vide infra*).

In the art field, terpenoid resins have been used as components for protective finishes and binding media of paintings and polychromed sculptures since ancient times [13,14]. In the latter, when used as a binding medium, natural resin is mixed with pigment, or is combined with drying oils and some organic or inorganic additive to form a suitable vehicle for pigment. Moreover, terpenoid resins are frequently included in recipes for varnishes to be used with toys, furniture, wagons and carriages, metals and swords, violins and musical instruments, gildings, etc. [15,16]. Many terpenoid plant resins have been used since ancient times, and their use has spread worldwide by means of commercial exchange which has been enhanced and extended. Examples may be found in varnishes and binding media based on colophony, Venice turpentine, sandarac, Manila copal, dammar, mastic or elemi resins, which have been prepared by artists from countries of the five continents. Besides, art objects may be found where terpenoid resins, endemic from specific geographical regions, are employed in the elabora-

* Corresponding author. Tel.: +34 963879312; fax: +34 963877319.
E-mail address: tdomenec@crbc.upv.es (M.T. Doménech-Carbó).

1387-3806/$ – see front matter © 2008 Elsevier B.V. All rights reserved.
doi:10.1016/j.ijms.2008.12.015

Fig. 1. *Jatobá* resin from *Hymenaea stigonocarpa* Mart. Peruaçu Valley, Minas Gerias, Brazil. Length of the divisions in the scale bar is 1 cm.

tion of local art objects. One such example is Mexican copals. They are triterpenoid resins obtained from some trees of the *Burseraceae* family, endemic in Mexico, and have been locally employed by Mexican painters as binding media in canvas and wall paintings [17].

Similarly, a number of works can be found in the literature related to the use of terpenoid resins which are endemic in Brazil for artistic purposes. For example, Souza and Avila [18] identified a terpenoid resin used as a protective varnish in Brazilian polychromed sculptures and paintings of the Baroque period by FTIR spectroscopy.

When applied as thin films of protective varnishes or as binding media in paint films, terpenoid resins undergo oxidative processes that alter their composition significantly compared to that of fresh or bulk material, which results in a notable change of the mechanical and optical properties of the film. Analytical studies have been done which not only deal with the characterization of the resins but also with their photochemical or thermal degradation. They have been performed by means of gas chromatography–mass spectrometry (GC–MS) [15,19-23], pyrolysis–GC–MS (Py–GC–MS) [24], thermally assisted hydrolysis and methylation–Py–GC–MS (THM–Py–GC–MS) [25–29] and on-line trimethylsilylation Py–GC–MS [17,30–32].

A number of studies have been reported in the scientific literature on the *Leguminosae* resins used as art materials [19,27,33–35]. Moreover, Class I fossil resins (ambers) are derived from the plant resins based primarily on polymers of labdatriene diterpenes. In many cases, a variety of related labdanoid precursors are incorporated into the developing polymeric structure to result in a final copolymeric structure which incorporates labdanoid carboxylic acids, alcohols and hydrocarbons [36–41]. Interestingly, the fossil resins from various Tertiary deposits in Mexico, Colombia and Brazil were derived from the *Hymenaea* genus [42]. With respect to uses of *Hymenaea* resins as art materials, Jácome reported that the use of a *Jatobá* resin in the manufacture of polychromed ceramics is mentioned in historical sources [43]. More recently, different authors [6,7,44] stated that the trunk resin of *Hymenaea* trees, in particular, the *Hymenaea courbaril* L., species, has been used in the manufacture of varnish in addition to medicinal applications.

This paper reports the results obtained in a study of the *Jatobá* resin collected from *Hymenaea stigonocarpa* Mart., which grows in the region of Minas Gerais (Brazil). For this purpose, methods based on GC–MS [17,22], THM–Py–GC–MS [25] using tetramethylammonium hydroxide (TMAH) as a derivatization reagent and on-line trimethylsilylation Py–GC–MS [17,32] using hexamethyldislylazane (HMDS) as a derivatization reagent have been applied and compared.

A second aim of this work has been the identification of the main chemical changes due to the degradation effect of light on the composition as one of the principal environmental ageing agents affecting the composition of the *Jatobá* resin when this material is prepared as a thin film for artistic applications. For this purpose, an accelerated UV light ageing process has been applied to a series of specimens of this resin prepared as thin films. In addition to the hyphenated MS techniques, FTIR spectroscopy was also applied in an attempt to obtain a more complete characterization of this resin. The optimization of a reliable and sensitive analysis method for the *Jatobá* resin will be valuable for future studies to assess the presence of this material in art objects and to investigate its possible influence on the behaviour of either the paint film or the protective varnish in the short or long term.

2. Experimental

2.1. Analytical reagents and reference materials

The reagents used to treat the samples and to prepare the specimens were: HMDS and methyl chloroformate (MCF) (purity 99%), absolute pyridine (Fluka, Buchs, Switzerland), chloroform (98% purity) for GC (Acros, Cambridge, USA), absolute methanol for analysis, sodium hydrogenocarbonate, TMAH (purity 99%) (Sigma–Aldrich, Steinheim, Germany) and acetone (Guinama, Valencia, Spain).

2.2. Natural resin samples

Jatobá resin (*Hymenaea stigonocarpa* Mart.), from the Peruaçu valley (Minas Gerais, Brazil), has been used for preparing the varnish model specimens.

2.3. Instrumentation

2.3.1. GC–MS

Experiments were carried out with an Agilent Technologies (Palo Alto, CA, USA) 6890N gas chromatograph equipped with an on-column injection system and coupled with an Agilent Technologies 5973N mass spectrometer. An HP-5MS capillary column (5% phenyl–95% methylpolysiloxane, 30 m × 0.25 mm I.D., 0.25 μm film thickness) was used.

The chromatographic conditions were as follows: a GC temperature of initially 100 °C then programmed at 5 °C min^{-1} to 295 °C, held for 8 min. The inlet was set at 250 °C. Samples were injected in the split mode (1:20 split ratio). The electronic pressure control was set to the constant flow mode with vacuum compensation. The helium gas flow was set at 1.3 mL min^{-1}.

Ions were generated by electron impact (EI) ionization (electron energy 70 eV) in the ionization chamber of the mass spectrometer. The mass spectrometer was scanned from m/z 20 to 800, with a cycle time of 1 s. The Agilent ChemStation software G1701CA MSD was used for GC–MS control, peak integration and mass spectra evaluation. The tuning of the mass spectrometer was carried out using perfluoro-tributylamine. Peak area (TIC) data were used to obtain the peak area percentage values. The temperatures of the interface and the source were 280 and 150 °C, respectively. Compounds were identified by using NIST and Wiley mass spectral libraries, and a third mass spectral library was created by the authors for the diterpenoid compounds.

2.3.2. Py–GC–MS

Experiments were carried out with an integrated system composed of a CDS Pyroprobe 1000 heated filament pyrolyzer (Ana-

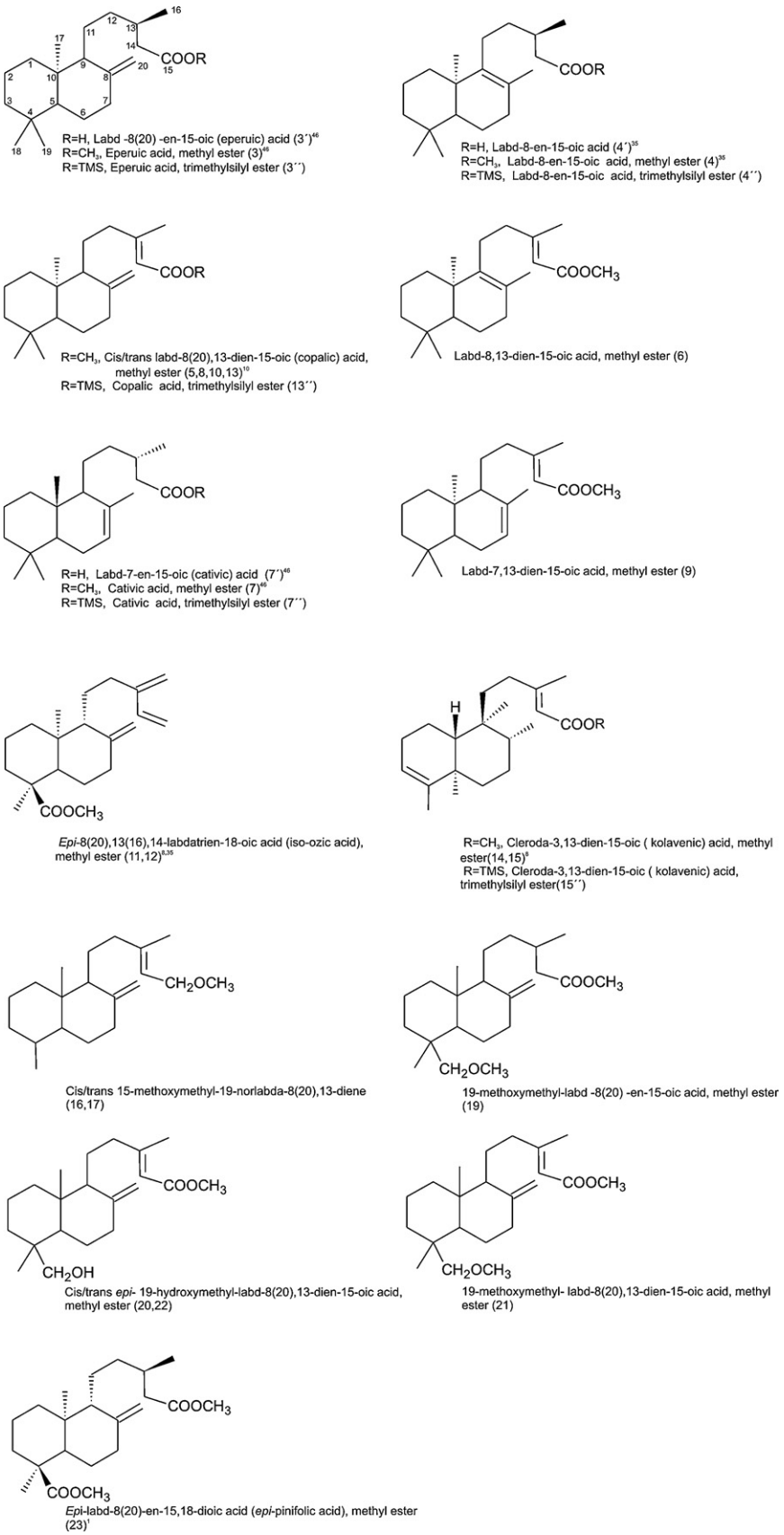

Fig. 2. Structure of the free *epi*-labdanoids identified in *Jatobá* resin and some secondary pyrolysis products formed by means of THM–GC–MS.

lytical Inc., New York, USA) and the GC–MS system described above. The aforementioned capillary column was used.

Pyrolysis was carried out using pre-calibrated Pt coil type pyrolyzers (CDS pyroprobe). The pyrolyzer interface and the inlet were set at 250 °C. Samples were injected in the split mode (split ratio 1:80). Chromatographic conditions were as follows: the initial temperature of 100 °C increased at 5 °C min^{-1} to 295 °C, where it was held for 8 min. The helium gas flow was set at 1.6 mL min^{-1}. The initial inlet pressure of the carrier gas was 72.5 kPa. The electronic pressure control was set to the constant flow mode with vacuum compensation.

2.3.3. FTIR spectroscopy

The ATR-IR spectra from specimens were obtained using a Vertex 70 Fourier transform infrared spectrometer equipped with an attenuated total reflection device and a FR-DTGS (fast recovery deuterated triglycine sulphate) temperature-stabilized coated detector. ATR crystal type: diamond. The range collected was 4000–500 cm^{-1}. The number of co-added scans was 32; resolution, 4 cm^{-1}.

2.4. Preparation of samples for GC–MS analysis

2.4.1. Off-line derivatization

The derivatization procedure was based on a methodology previously developed in our laboratory for the analysis of diterpenoid resins [17]. Samples from the solid resin and the thin film specimens in the range 20–10 μg were dissolved in 50 μL methanol–pyridine (4:1, v/v). Then, 10 μL MCF was added. The reaction mixture was vortexed for around 10 s and the derivatives were extracted in 50 μL chloroform containing 1% MCF. Next, 50 μL of a saturated solution of $NaHCO_3$ were added and the mixture was carefully shaken. A 1 μL aliquot of the organic phase was injected into the GC–MS system.

2.5. Preparation of samples for Py–GC–MS analysis

2.5.1. On-line THM

Samples were directly pyrolyzed to obtain the chromatograms (pyrograms) of the resins. 1–10 μg of sample extracted from the test specimen were placed into a quartz tube for pyrolysis with 10 μL of 25% TMAH aqueous solution, and positioned in the platinum coil probe, which was then inserted into the interface. Then, samples were pyrolyzed at 600 °C for 10 s.

2.5.2. On-line trimethylsilylation

Samples were directly pyrolyzed to obtain the chromatograms (pyrograms) of the resins. 1–10 μg of sample extracted from the test specimen was placed in a quartz tube for pyrolysis with 0.5 μL of HMDS and positioned in the platinum coil probe, which was then inserted into the interface. After this, samples were pyrolyzed at 650 °C for 10 s.

2.5.3. Selection of the pyrolysis temperature

The influence of temperature on the pyrolysis product distribution of the studied resin was considered in a series of experiments. According to Anderson and Winans [36], when pyrolysis of diterpenoid resins was performed with TMAH over 540 °C, the relative abundance of secondary pyrolysis products increased considerably. Nevertheless, experiments carried out in our laboratory to optimize the pyrolysis conditions showed no significant differences in the

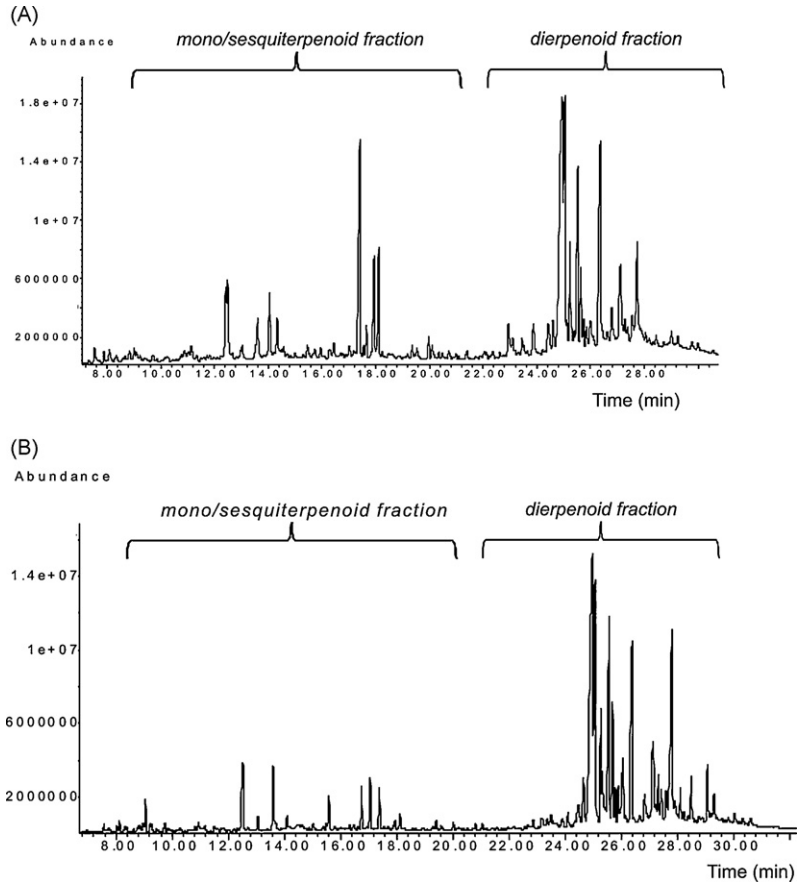

Fig. 3. Pyrogram of methyl ester derivatives corresponding to a sample excised from a fragment of *Jatobá* resin analyzed by means of THM–GC–MS: (A) pyrolysis at 480 °C for 10 s; (B) pyrolysis at 650 °C for 10 s.

Table 1
Assignment of methyl ester derivatives, molecular mass, retention time and main fragment ions corresponding to a sample excised from a fragment of *Jatobá* resin and analysed by means of THM–GC–MS.

Peak	Diterpenoid fraction assignment	M_w	t_r (min)	Mass spectra data (70 eV) Characteristic ions[a]: *m*/*z*
1	Unidentified labdane	318?	24.47	95, 105,**119**, 189, 191, 277, 305, 318
2	Unidentified labdane	318	24.67	95,**121**, 191, 241,257, 301
3	Labd-8(20)-en-15-oic acid (eperuic acid), methyl ester	320	24.98	**137**,177,191,277,289,305,320
4	Labd-8-en-15-oic acid, methyl ester[b]	320	25.08	95,**191**,277,289,305,320
5	*Cis/trans* Labd-8(20),13-dien-15-oic acid (copalic acid), methyl ester	318	25.29	55,69,81,95,109,**114**,121,137,205,287,303,318
6	Labd-8,13-dien-15-oic acid, methyl ester[b]	318	25.34	55,69,95,109,121,135,**191**,287,303,318
7	Labd-7-en-15-oic acid (cativic acid), methyl ester	320	25.58	55,69,81,95,109,122,**191**,196,277,289,305,320
8	Isomer of compound **5**[b]	318	25.70	55,69,81,**95**,107,121,137,191,217,244,287,**303**,318
9	Labd-7,13-dien-15-oic acid, methyl ester	318	25.80	95,107,121,135,**189**,191,286,303,318
10	Isomer of compound **5**[b]	318	25.90	81,109,114,**205**,303,318
11	Isomer of compound **12**[b]	316	26.04	95,109,121,135,**191**,301,316
12	*Epi*-8(20),13(16),14-labdatrien-18-oic acid (iso-ozic acid), methyl ester	316	26.07	95,109,**121**,135,175,191,241,257,287,301,316
13	*Cis/trans* labd-8(20),13-dien-15-oic acid (copalic acid), methyl ester	318	26.39	55,69,81,95,109,**114**,121,137,205,287,303,318
14	Isomer of compound **15**[b]	318	26.85	81,95,109,135,189,**205**,301
15	Cleroda-3,13-dien-15-oic acid (kolavenic acid), methyl ester	318	27.14	81,95,109,135,**189**,204,205
16	*Cis/trans* 15-methoxymethyl-19-norlabda-8(20),13-diene[b]	290	27.33	**98**,123,189
17	*Cis/trans* 15-methoxymethyl-19-norlabda-8(20),13-diene[b]	290	27.44	**98**,123,189
18	Unidentified labdane	–	27.61	95,109,**123**,191,209,362
19	19-Methoxymethyl-labd-8(20)-en-15-oic acid, methyl ester	350	27.81	121,135,149,175,223,**305**,318
20	*Cis/trans epi*-19-hydroxymethyl-labd-8(20),13-dien-15-oic acid, methyl ester	334	28.11	107,121,135,189,302,271,**303**,333,334
21	19-Methoxymethyl-labd-8(20),13-dien-15-oic acid, methyl ester	348	28.50	81,95,107,121,175,189,274,**303**,348
22	*Cis/trans epi*-19-hydroxymethyl-labd-8(20),13-dien-15-oic acid, methyl ester	334	29.08	107,121,135,189,302,271,**303**,333,334
23	*Epi*-labd-8(20)-en-15,18-dioic acid (*epi*-pinifolic acid), dimethyl ester	364	29.32	**121**,304,305,364

? signifies that the molecular weight has been tentatively assigned.
[a] Base peak in bold.
[b] Assignment of structure based on the fragment ion pattern in the mass spectrum.

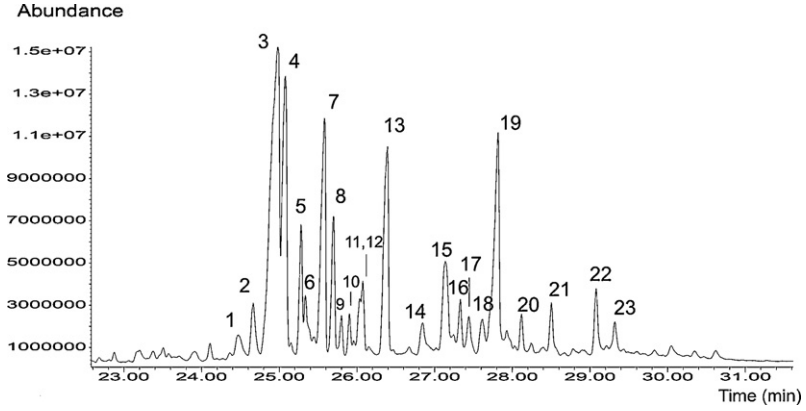

Fig. 4. Detail of the diterpenoid fraction appearing in the pyrogram of methyl ester derivatives corresponding to a sample excised from a fragment of *Jatobá* resin analyzed by means of THM–GC–MS.

diterpenoid fraction of the resin with pyrolysis at either 480 °C (the optimal pyrolysis temperature proposed by Anderson and Winans [36]) or 650 °C. Fig. 3A shows the pyrogram of a sample of *Jatobá* resin performed at 480 °C. It should be noted that a higher level of residual materials was observed in the quartz tube after pyrolysis at this temperature when compared with pyrolysis performed at 650 °C. Analyses done at 650 °C (Fig. 3B) showed a decrease in the intensity of the peaks corresponding to the mono-, sesquiter-

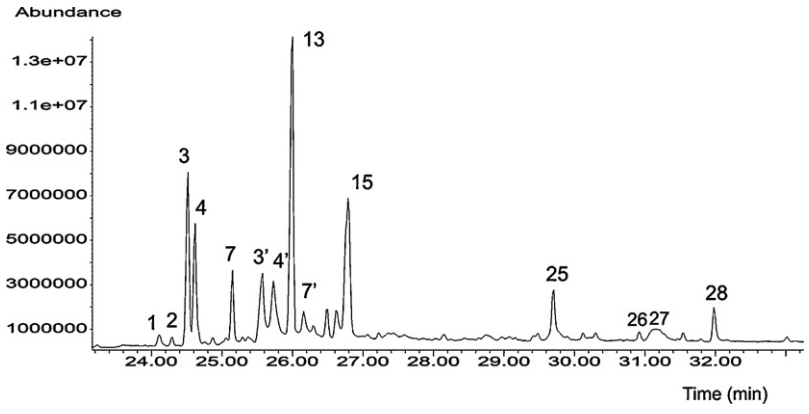

Fig. 5. Chromatogram of methyl ester derivatives corresponding to a sample excised from a fragment of *Jatobá* resin using GC–MS with MCF derivatization.

penoid fraction, whereas a close distribution of peaks to that at 480 °C was noted in the diterpenoid fraction. Thus, the distribution of the products observed was very similar, which allows us to conclude that the pyrolysis temperature within the studied range does not significantly affect the presence and relative abundances of the compounds obtained. Therefore, this last temperature was finally selected for carrying out the study on *Jatobá* resin. This is consistent with temperatures in the range 600–650 °C that have been used in other studies of organic compounds present in artworks, particularly diterpenoid resins [24,26,27,29–31].

2.6. Preparation of test specimens

10 g of *Jatobá* resin was dissolved in 100 mL acetone. A series of specimens was prepared by spreading the resulting solution onto glass slides (average thickness, 50–80 μm). Specimens were stored at room temperature for two months and were subsequently analyzed.

A number of the specimens was artificially light-aged to approximate a natural photoageing effect on the chemical composition of the resin. UV light ageing consisted of irradiating samples in a Dycometal model QUV-Basic chamber provided with a UVB-313EL UV lamp (Q-Panel Lab Products), which produces mostly short-wave UV light with a maximum intensity at ca. 310 nm, the equivalent to a 40 W fluorescent lamp. The temperature was maintained at a constant value of 45 °C. Specimens were exposed to UV light for 720 h.

3. Results and discussion

3.1. Analysis of unaged pure resin specimens

3.1.1. Solid resin

GC–MS and Py–GC–MS analyses of samples excised from the opaque pale-yellow pieces of *Jatobá* resin (see Fig. 1) generally showed a small sesquiterpenoid fraction which was mainly composed of caryophyllene oxide. The diterpenoid fraction of this resin consists of a number of *epi*-labdanes which are listed in Table 1 (see also Fig. 2). The most intense peaks appear in the pyrogram depicted in Fig. 4, which was obtained by means THM–Py–GC–MS, and they correspond to the methyl ester derivatives of eperuic acid (3), and to its Δ7 (7) and Δ8 (4) isomers, as well as to the *cis*/*trans* isomers of copalic acid (5,13) and Δ7 (9), Δ8 (6), and other (8) isomers

Table 2
Assignment of methyl ester and trimethylsilyl derivatives and molecular mass corresponding to a sample excised from a fragment of *Jatobá* resin analysed by means of THM–GC–MS, on line trimethylsilylation Py–GC–MS and off line methylation GC–MS.

Peak	Diterpenoid fraction assignment	Mw	THM–GC–MS	On line trimethylsilylation Py–GC–MS	Off line methylation GC–MS
1	Unidentified labdanoid[a]	318?	√	–	√
2	Unidentified labdanoid[a]	318	√	–	√
3	Labd-8(20)-en-15-oic acid (eperuic acid), methyl ester[a]	320	√	–	√
3′	Labd-8(20)-en-15-oic acid (eperuic acid)[a]	306	–	–	√
3″	Labd-8(20)-en-15-oic acid (eperuic acid), TMS ester[a]	378	–	√	–
4	Labd-8-en-15-oic acid, methyl ester[a]	320	√	–	√
4′	Labd-8-en-15-oic acid[a]	306	–	–	√
4″	Labd-8-en-15-oic acid, TMS ester[a]	378	–	√	–
5	*Cis/trans* labd-8(20),13-dien-15-oic acid (copalic acid), methyl ester[b]	318	√	–	–
6	Labd-8,13-dien-15-oic acid, methyl ester[b]	318	√	–	–
7	Labd-7-en-15-oic acid (cativic acid), methyl ester[a]	320	√	–	√
7′	Labd-7-en-15-oic acid (cativic acid)[a]	306	–	–	√
7″	Labd-7-en-15-oic acid (cativic acid), TMS ester[a]	378	–	√	–
8	Isomer of compound **5**[c,b]	318	√	–	–
9	Labd-7,13-dien-15-oic acid, methyl esterd	318	√	–	–
10	Isomer of compound **5**[c,b]	318	√	–	–
11	Isomer of compound **12**[c,b]	316	√	–	–
12	Epimer-8(20),13(16),14-labdatrien-18-oic acid (iso-ozic acid), methyl ester[a]	316	√	–	–
13	*Cis/trans* Labd-8(20),13-dien-15-oic acid (copalic acid), methyl ester[a]	318	√	–	√
13″	*Cis/trans* Labd-8(20),13-dien-15-oic acid (copalic acid), TMS ester[a]	376	–	√	–
14	Isomer of compound **15**[c,b]	336	√	–	–
15	Cleroda-3,13-dien-15-oic acid (kolavenic acid), methyl ester[a]	336	√	–	√
15″	Cleroda-3,13-dien-15-oic acid (kolavenic acid), TMS ester[a]	376	–	√	–
16	*Cis/trans* 15-methoxymethyl-19-norlabda-8(20),13-diene[b]	290	√	–	–
17	*Cis/trans* 15-methoxymethyl-19-norlabda-8(20),13-diene[b]	290	√	–	–
18	Unidentified labdanoid[b]	–	√	–	–
19	19-Methoxymethyl-labd-8(20)-en-15-oic acid, methyl ester[b]	350	√	–	–
20	*Cis/trans epi*-19-hydroxymethyl-labd-8(20),13-dien-15-oic acid, methyl ester[b]	334	√	–	–
21	19-Methoxymethyl-labd-8(20),13-dien-15-oic acid, methyl ester[b]	348	√	–	–
22	*Cis/trans epi*-19-hydroxymethyl-labd-8(20),13-dien-15-oic acid, methyl ester[b]	334	√	–	–
23	*Epi*-labd-8(20)-en-15,18-dioic acid (*epi*-pinifolic acid), methyl ester[a]	364	√	–	–
24″	Unidentified labdanoid, TMS ester[d]	392	–	√	–
25	Unidentified labdanoid [d]	334	–	–	√
25″	Unidentified labdanoid, TMS ester [d]	392	–	√	–
26	Unidentified labdanoid [d]	334	–	–	√
26″	Unidentified labdanoid, TMS ester [d]	392	–	√	–
27	Unidentified labdanoid [d]	332	–	–	√
28	Unidentified labdanoid [d]	–	–	–	√
28″	Unidentified labdanoid, TMS ester[d]	–	–	√	–

? signifies that the molecular weight has been tentatively assigned.
[a] Free diterpenoid from the resin.
[b] Secondary pyrolysis yield.
[c] Assignment of structure based on the fragment ion pattern in the mass spectrum.
[d] Oxidized diterpenoid from the resin.

Table 3
Characteristic fragment ions and *m*/*z* values of methyl ester derivatives of *epi*-labdanoid acids formed by means of THM–GC–MS.

Compound	3	4	6	7	12	13	15	23
$M^{+\bullet}$	320	320	318	320	316	318	318	364
$[M\text{-}CH_3]^+$	305	305	303	305	301	303	303	–
$[M\text{-}OCH_3]^+$	289	289	287	289	–	287	–	–
$[M\text{-}CH_3OH]^+$	–	–	–	–	–	286	–	–
$[M\text{-}CH_3\text{-}CO]^+$	277	277	–	277	–	–	–	–
$[M\text{-}COOCH_3]^+$	–	–	–	–	257	–	–	–
$[M\text{-}CH_3OH\text{-}CO]^+$	–	–	–	–	256	258	–	304
$[M\text{-}HCOOCH_3\text{-}CH_3]^+$	–	–	–	–	241	–	–	–
i	137	–	–	–	–	137	121	181
i-H $COOCH_3$	–	–	–	–	–	–	–	121
ii	–	–	–	–	–	205	205	–
iii	–	–	–	–	–	189	189	189
iv	191	–	–	–	–	–	–	235
iv-HR_1	175	–	–	175	175	–	–	175
v-CH_3	–	109	109	109	–	–	–	–
vi	–	–	–	196	–	–	–	–
vi-CH_3-$COOCH_3$	–	–	–	122	–	–	–	–
vii	–	191	191	191	–	–	–	–

[10]. Methyl ester derivatives of iso-ozic acid (12) and kolavenic acid (15) are present but to a lesser extent along with *epi*-pinifolic diacid (23). Additionally, a number of compounds belonging to the *epi*-labdanoid series have tentatively been identified according to their fragment ion pattern from their mass spectra, namely, *cis/trans* isomers of 15-methoxymethyl-19-norlabda-8(20),13-diene (16,17), 19-methoxymethyl-labd-8(20)-en-15-oic acid (19), methyl ester of *cis/trans* isomers of *epi*-19-hydroxymethyl-labd-8(20),13-dien-15-oic acid (20,22) and 19-methoxymethyl-labd-8(20),13-dien-15-oic acid (21). Finally, small amounts of a number of unidentified compounds appear in the pyrogram which have been assigned to the *epi*-labdanoid series in accordance with their fragmentation pattern.

GC–MS analyses performed on samples of the solid resin using MCF as a derivatization reagent provided simpler chromatograms, including the most abundant compounds found in the THM–GC–MS mode, as illustrated in Fig. 5 and summarized in Table 2: methyl esters of eperuic acid (3) and its Δ7 (7) and Δ8 (4) isomers, along with copalic acid (13) and kolavenic acid (15). Additionally, the peaks of underivatized eperuic acid (3′), its Δ7 (7′) and Δ8 (4′) isomers have been identified in the chromatogram, suggesting that this reagent is less effective than TMAH on pyrolysis to accomplish a complete derivatization of the compounds conforming the *Jatobá* resin.

On-line derivatization with HMDS in the Py–GC–MS mode also provided a simpler pyrogram (see Table 2). Trimethylsilyl esters (TMS) of eperuic acid (3″) and its Δ7 (7″) and Δ8 (4″) isomers, copalic acid (13″) and kolavenic acid (15″), have been identified by this analytical method. Additionally, a number of unidentified *epi*-labdanoids appear in the pyrogram.

This composition differs from that found in studies of other *Hymenaea* resins growing in this Amazonian region [1,6,9] or in African regions [11,45]. The composition of the *Jatobá* resin also differs from that found in other *Leguminosae* resins used in art such as copals [33–35] and copaiba balsam [27].

Secondary pyrolysis reactions undergone by free diterpenoids, such as fragmentation, cleavage of hydrolysable bonds, isomerization, dehydration and recombination due to the strong alkalinity of the TMAH solution, have been described in the analysis of diterpenoid resins from the *Pinaceae* species used as art materials [29]. Comparing the results obtained from the three analytical methods applied enabled us to recognize these reactions taking place during the pyrolysis process of the *Jatobá* resin when THM–GC–MS was used. Thus, discrimination between the real components of the analyzed resin and their isomers or secondary pyrolysis products could be established, as summarized in Table 2.

Table 3 summarizes the main fragment ions identified in the mass spectra of the free *epi*-labdanoids occurring in the ana-

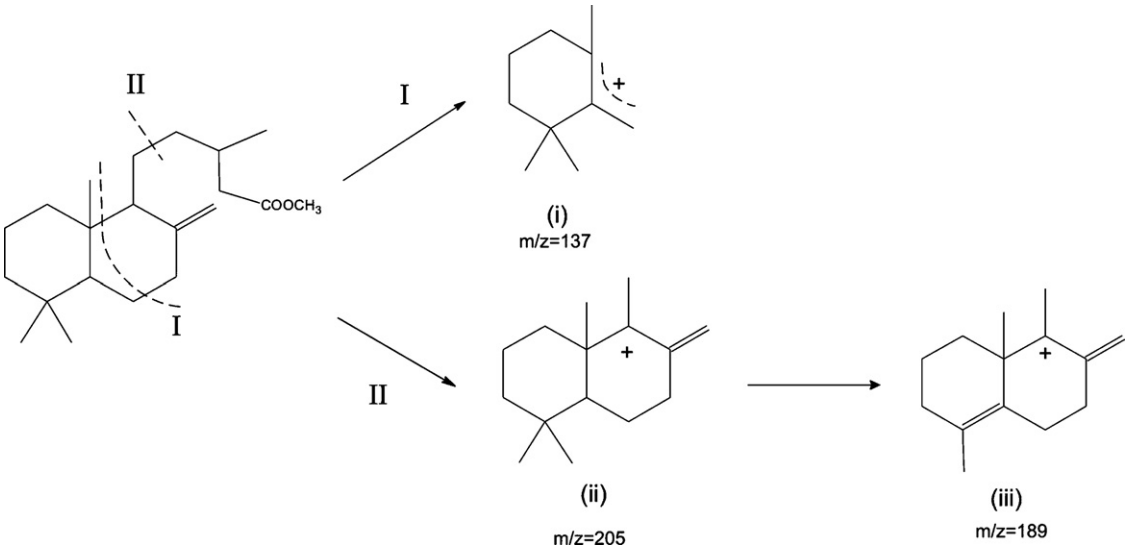

Fig. 6. Structure and formation of fragment ions i–iii from *epi*-labdanoid molecules.

Table 4
Characteristic fragment ions and *m*/*z* values of secondary pyrolysis products of *epi*-labdanoid acids formed by means of THM–GC–MS.

Compound	9	16	17	19	20	21	22
$M^{+\bullet}$	318	290	290	350	334	348	334
$[M\text{-}CH_3]^+$	303	–	–	335	319	333	319
$[M\text{-}OCH_3]^+$	287	–	–	–	–	–	–
$[M\text{-}CH_2OH]^+$	–	–	–	–	303	–	303
$[M\text{-}CH_2OCH_3]^+$	–	–	–	305	–	–	–
I	–	123	123	–	–	167	–
i – H_2O	–	–	–	149	135	149	–
i – CH_3OH	–	–	–	135	121	135	121
i – $HCH_2O\ CH_3$	–	–	–	121	–	121	–
ii	–	–	–	–	221	–	221
ii– H_2O	–	–	–	–	203	–	203
iii	–	189	189	189	189	189	189
iv	–	–	–	221	207	221	207
iv-HR_1	–	–	–	175	175	175	175
v– CH_3	109	–	–	–	–	–	–
vii	191	–	–	–	–	–	–
viii-CH_4	189	–	–	–	–	–	–

lyzed resin. Different fragmentation pathways can be distinguished depending on the position of the carboxylic group in a similar way to that found for labdanoid series [26], or to the number and position of double bonds in the rings and side chain [46]. Interestingly, most of the compounds identified exhibit a C(8)–C(20) double bond (eperuic acid, copalic acid, etc.). Their mass spectra are characterized by the appearance of the molecular ion together with peaks corresponding to methyl elimination and, in some cases, to a loss of the side chain. The presence of the carboxylic group in the side chain enhances the elimination of methyl $[M\text{-}CH_3]^+$, methoxy $[M\text{-}OCH_3]^+$ and sometimes, methanol $[M\text{-}CH_3OH]^+$ groups, which is frequently followed by a loss of CO, resulting in fragment ions $[M\text{-}CH_3OH\text{-}CO]^+$ and $[M\text{-}CH_3\text{-}CO]^+$. Cleavage of the C(6)–C(7) and C(9)–C(10) allylic bonds, followed by the elimination of hydrogen, appear to be the favoured reaction for the majority of this type of compounds, resulting in ion i (Fig. 6) [47,48]. The corresponding peak is, in general, significant and, in most cases, the base peak [46]. When the substituent at C(4) is a methyl ester ($R = COOCH_3$), as in *epi*-pinifolic acid (23), ion i may also lose this substituent together with hydrogen. This gives an i-$HCOOCH_3$ ion which results in a strong peak at *m*/*z* 121 which, in this case, is the base peak [48]. Similarly, the presence of a-CH_2OCH_3 or carbinol group as a substituent at C(4), as with compounds (19) and (21) and (20) and (22) (*vide infra*), leads to the elimination of water or methanol from the previously formed fragment i (see Table 4).

A second fragmentation pathway consists in the cleavage of the C(11)–C(12) bond, which yields fragment ion ii and, in turn, results in fragment iii from the loss of the functional group in C(4) (see Fig. 6). This reaction occurs without a hydrogen transfer in the compounds identified, which do not exhibit hydroxyl groups in the side chain. As Enzell and Ryhage described [46], a 1,2-shift of the C(9) hydrogen to C(11) takes place during the formation of ion ii since this increases the stability of the formed ion ii. Ion ii is capable of undergoing further reactions. Thus, ion ii eliminates HR (where R is the substituent in C(4)) to form ion iii, as shown in Fig. 6. When there is a $R = CH_2OH$ substituent in C(4), ion ii eliminates water resulting in ion ii-H_2O. In compounds with a double bond in C(13)–C(14), such as copalic acid, the C(9) hydrogen atom is transferred to C(14) by a six-member ring mechanism [10,49].

A peak at 114 *m*/*z* is due to an ion formed by the cleavage of the C(11)–C(12) bond and the transfer of the C(9) hydrogen to the smaller fragment by means of a six-membered ring mechanism [10].

The cleavage of the C(9)–C(11) bond can also take place in the identified compounds without a hydrogen transfer to the larger fragment to result in ion iv. The resulting ion can lose one of its substituents to result in ion iv-HR_1 (see Fig. 7) [46].

Mass spectra of compounds with a C(7)–C(8) double bond, such as cativic acid (7), are dominated by the ions formed from a retro-Diels Alder-type reaction resulting in the formation of ions of types v and vi (Fig. 8). Ion v further eliminates a methyl group, whereas ion vi can eliminate a methanol, methyl formate and methyl acetate group. Peaks due to the cleavage of the C(9)–C(11) bond with the formation of ion vii (Fig. 9A) are also significant in the mass spectra of these compounds [46]. If the compound has a C(13)–C(14) double bond, β-cleavage of this double bond in C(13) yields to $[M\text{-}113]^+$ ion viii (Fig. 9B). This last ion can eliminate CH_4 in C(4).

Interestingly, a number of compounds appeared in the THM–GC–MS pyrogram associated with secondary pyrolysis pro-

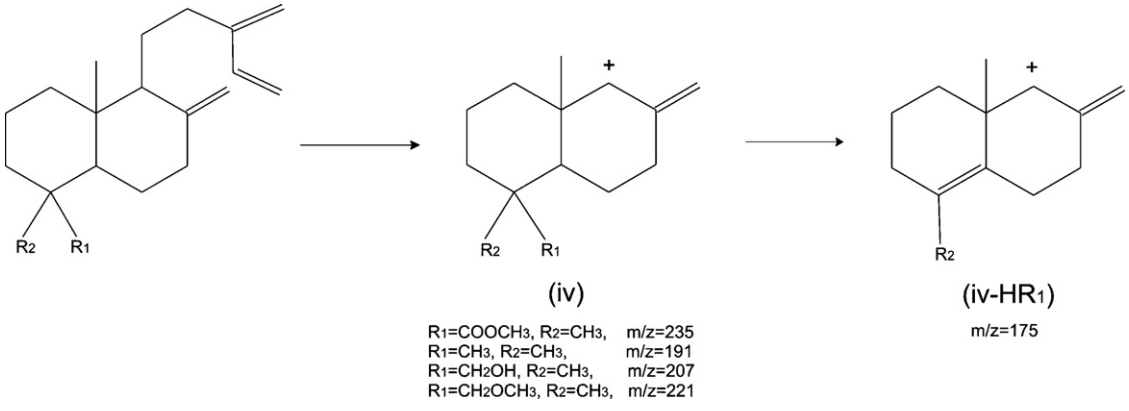

Fig. 7. Structure and formation of fragment ion iv from *epi*-labdanoid molecules.

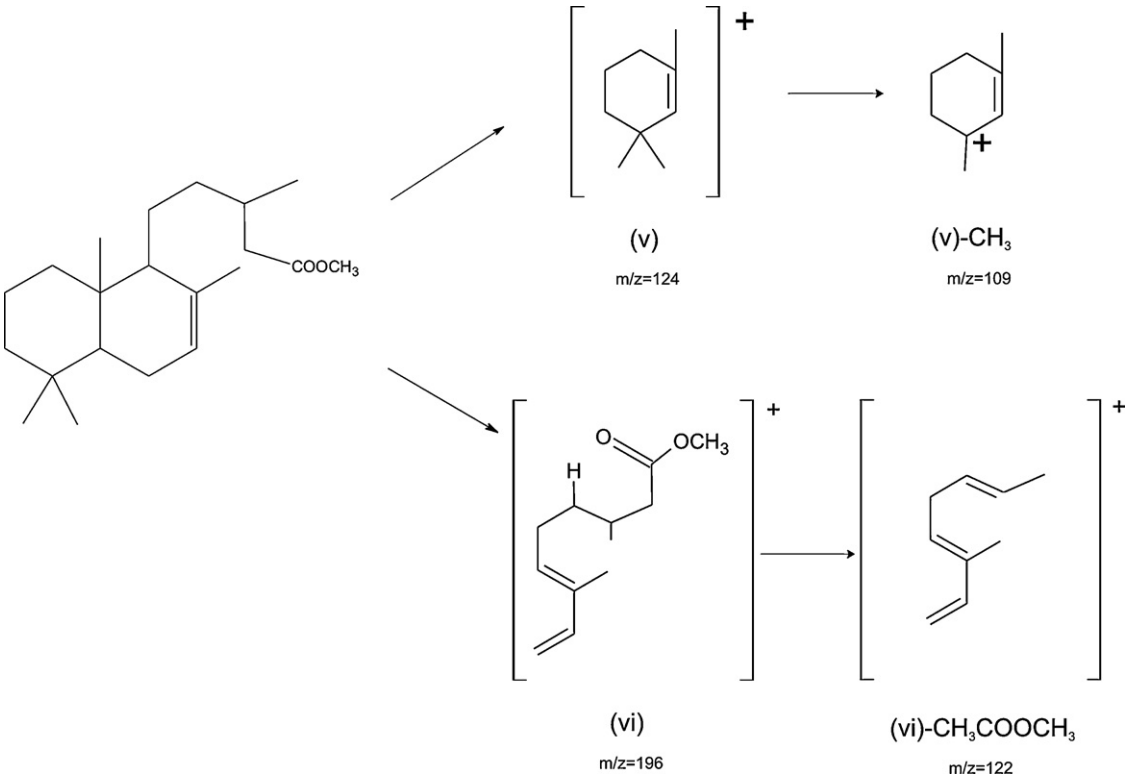

Fig. 8. Structure and formation of fragment ion v and vi from *epi*-labdanoid molecules.

cesses involving the substitution of the methyl group in C4 by H (16,17), CH_2OCH_3 (19,21) and CH_2OH (20,22). Table 4 summarizes the main fragment ions and *m*/*z* values of these secondary pyrolysis products formed during the THM–GC–MS analysis.

No pyrolysis products of the polymeric fraction appeared in the analyses performed, which is in good agreement with the high solubility exhibited by fresh *Jatobá* resin in acetone. This was reported in early studies on other *Hymenaea* species [35] and contrasts with the behaviour exhibited by resins from other *Leguminosae* families, in which ozic acid, present to a large extent, is responsible for their high degree of polymerization. Acids of the ozic series are the epimers of the communic series, except for the carboxylic group, which is equatorial rather than axial. The polymer formed from this compound is more highly cross-linked than polycommunic acid [35].

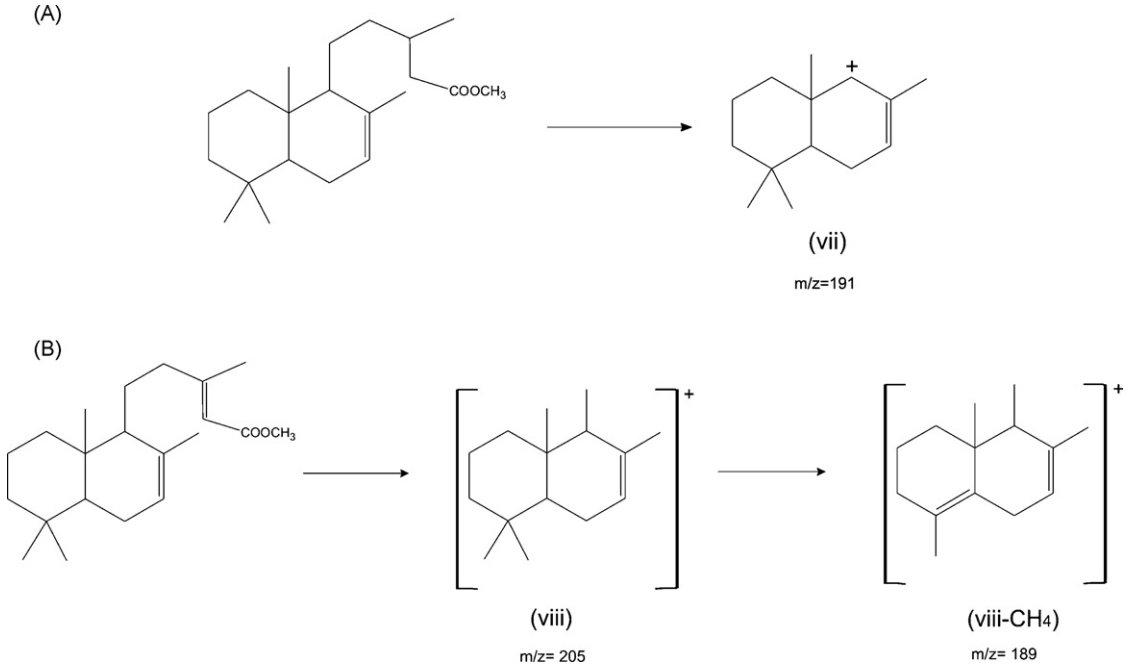

Fig. 9. Structure and formation of fragment ion vii from *epi*-labdanoid molecules.

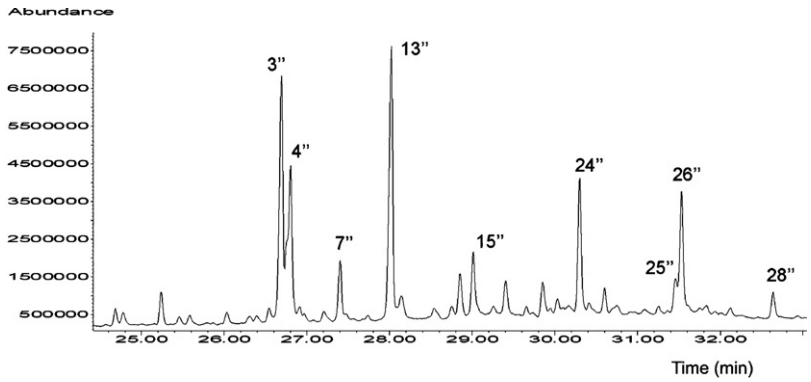

Fig. 10. Pyrogram of TMS ester derivatives corresponding to a sample from the unaged thin film specimen.

3.1.2. Thin film specimens

A similar distribution of peaks to that found in the bulk resin is observed in the samples excised from the resin prepared as a thin film, except for the significant increase of the intensity of some peaks appearing at higher retention times in the chromatogram obtained from both the MCF off-line and the HMDS on-line derivatizations (Fig. 10). Some of the compounds (24–28) exhibited molecular ions of 332 and 334 (methyl derivatives) and characteristic fragment ions $[M\text{-}CH_3]^+$ and $[M\text{-}CH_3OH]^+$ associated with methanol loss, so that they could tentatively be associated with oxidized derivatives of the original *epi*-labdanoids bearing ketone or hydroxyl groups, formed as result of the oxidation processes taking place during this initial ageing process in which the specimens were not exposed to an intense source of UV radiation. This hypothesis is supported by the significant increase of IR absorption bands appearing at 3300 and 1021 cm^{-1} and ascribed to stretching vibrations of the OH and C-O groups of alcohols, respectively, as seen in Fig. 11.

3.2. Analysis of UV light-aged specimens

The analysis performed on UV light-aged specimens demonstrates that *epi*-labdanoids undergo similar degradation processes on exposure to UV radiation to those observed in other *Leguminosae* resins [26].

The chromatograms and pyrograms obtained from thin film specimens of resin subjected to an intense source of UV light showed some changes that can be recognized by comparing the normalized peak area value N of the i *epi*-labdanoid compounds and their oxidation products obtained before and after ageing. The normalized peak area value N_i of a specific compound is defined as:

$$N_i = 100 \times \left(\frac{A_i}{\sum A_i} \right),$$

where A_i is the peak area of this specific compound i appearing in the pyrogram. Peak area values used for calculating the corresponding normalized peak area values are the average obtained from three replicate analyses from each specimen studied. In general, acceptable repeatability was obtained under the experimental conditions applied, indicated by values obtained for the relative standard deviation of the normalized peak area in the 2–4% range. Fig. 12 shows the bar chart summarizing the normalized values of the peak area of the free *epi*-labdanoids composing the unaged thin film and the UV light-aged thin film of *Jatobá* resin. Normalization has been carried out by considering all the eperuic acids (8(20), Δ7 and Δ8 isomers), kolavenic acid, copalic acid and labdanoids (24″), (26″) and (28″) as the compounds exhibiting the more prominent peaks in the pyrogram. It is interesting to note that the relative content of copalic and eperuic acid varies with UV light ageing for an increase in the total content of eperuic acid to take place in parallel to a decrease in the content of copalic acid. In contrast, no significant changes in the N_i value of the oxidized *epi*-labdanoids (24″–28″) appearing at higher retention time were observed.

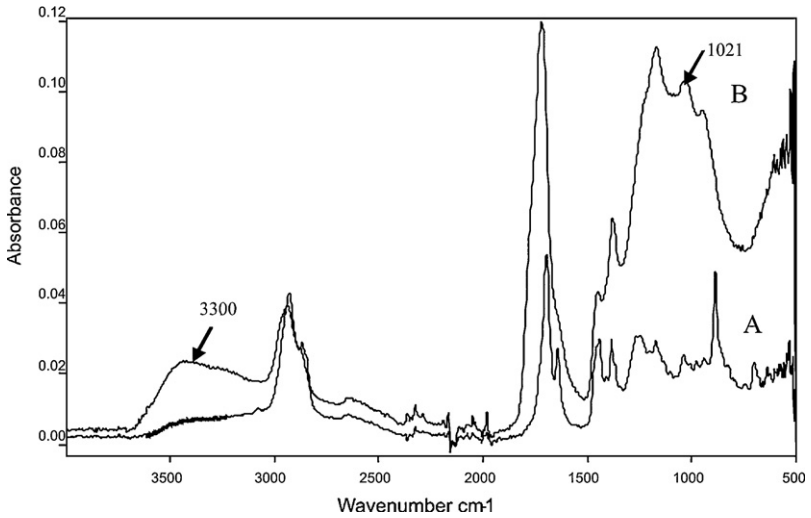

Fig. 11. IR absorption spectra corresponding to: (A) *Jatobá* resin pieces and (B) UV light aged for 720 h.

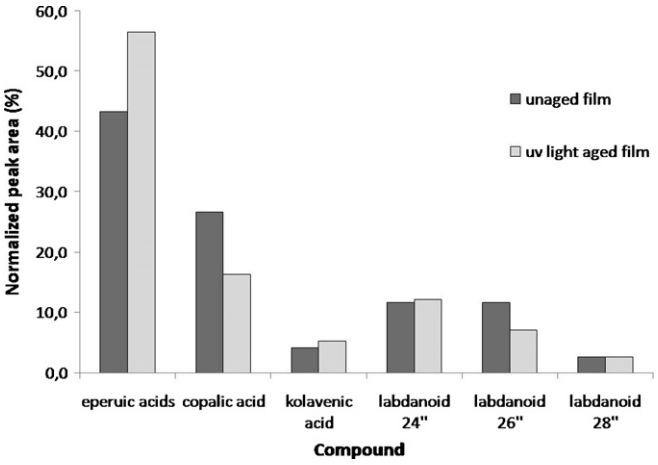

Fig. 12. Bar chart corresponding to the normalized values of the peak area for the free labdanoids composing the unaged thin film and the UV light-aged thin film specimens of *Jatobá* resin.

Changes in the relative content of the different isomers of eperuic acid, the main *epi*-labdanoid detected in *Jatobá* resin have also been observed. Fig. 13 illustrates the bar chart corresponding to the normalized values of the peak area for the TMS derivatives of eperuic acid and its Δ7 and Δ8 isomers which compose the solid resin, the unaged thin film and the UV light-aged thin film specimens. This diagram shows that eperuic acid content increases from the solid fragment of resin to the unaged and UV light-aged thin film. The proportion of the Δ8 isomer is relatively unchanged in the solid resin. In contrast, Δ7 isomer (cativic acid) shows a remarkable decrease from the solid fragment of resin to the unaged thin film, and a similar value to that from the unaged thin film is observed in the UV light-aged sample. This behaviour was consistent in the different replicates analyzed.

Another interesting finding is the appearance of a shoulder of the peak of the Δ8 isomer of eperuic acid at 26.75 min in the pyrogram corresponding to the unaged thin film (Fig. 14a), which appears as a new peak that is well resolved in the pyrogram of the UV light-aged film (Fig. 14b), and has been attributed to the promotion of isomerization reactions in this resin due to the UV light. The mass spectrum obtained from this new peak was similar to that from eperuic acid (Fig. 14c). These observations could be important for the detection of aged samples of the resin in artefacts. However, the reason for the chemical change is unclear and requires further study.

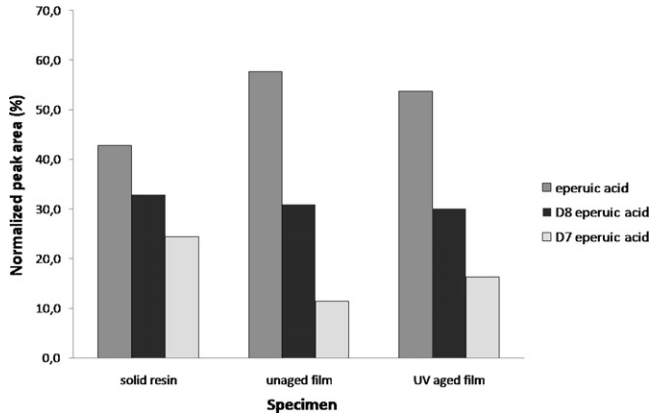

Fig. 13. Bar chart corresponding to the normalized values of the peak area for the TMS derivatives of eperuic acid and its Δ7 and Δ8 isomers composing the solid resin, the unaged thin film and the UV light-aged thin film specimens.

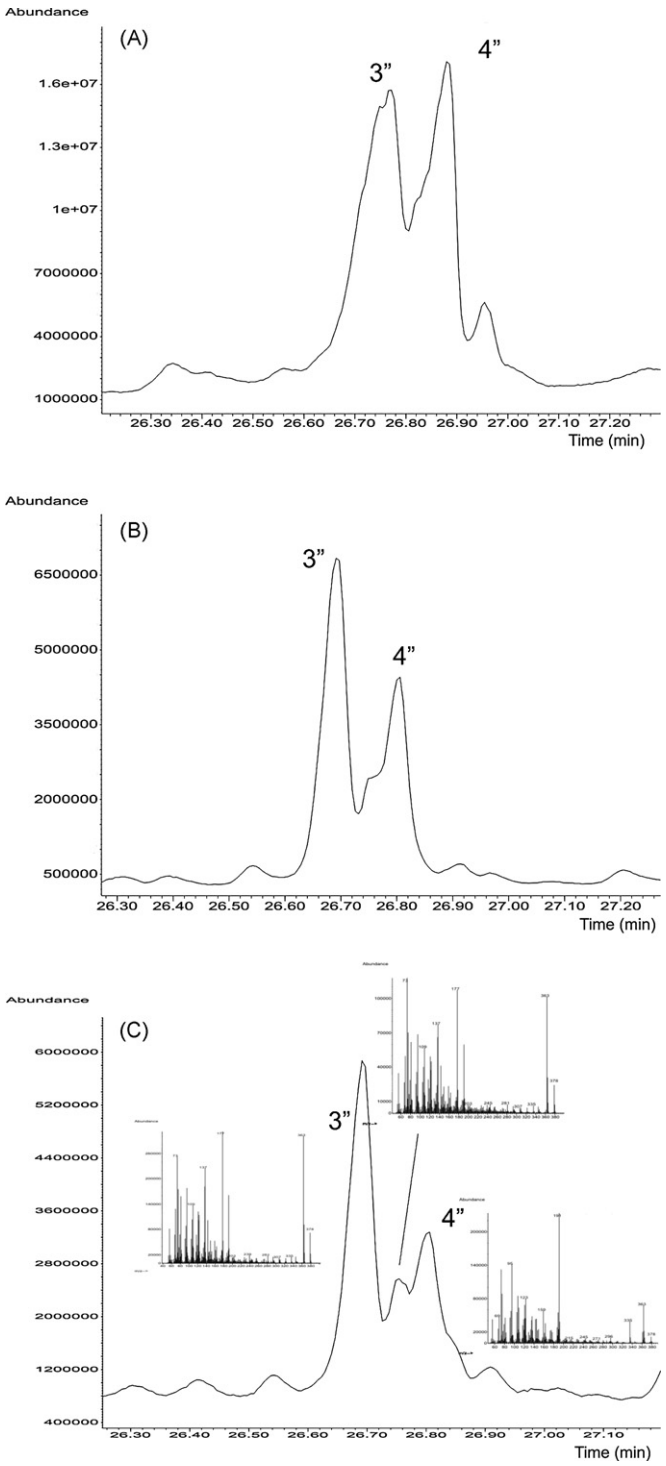

Fig. 14. (A) Detail of the shoulder appearing in the Δ8 eperuic acid peak from the pyrogram obtained with HMDS from the unaged thin film specimen. (B) Detail of the well resolved peak appearing between the eperuic acid and the Δ8 eperuic acid peak from the pyrogram obtained with HMDS from the UV light-aged thin film specimen, which is ascribed to a new isomer of the eperuic acid due to the effect of UV light. (C) Mass spectra of: eperuic acid (left), new isomer of eperuic acid (top) and Δ8 eperuic acid (right).

No polymeric fraction or pyrolysis fragments of the polymeric fraction were found from the pyrograms performed on UV light-aged specimens confirming the low tendency of this resin to polymerize. This is a factor which may enable it to be distinguished from other *Leguminosae* resins.

4. Conclusions

This study has identified the main compounds present in *Jatobá* resin collected from *Hymenaea stigonocarpa* Mart. Eperuic acid and its $\Delta 7$ (cativic acid) and $\Delta 8$ isomers, together with copalic acid, are the major components of the resin. Other compounds such as kolavenic acid, iso-ozic acid and *epi*-pinifolic acid have also been identified, present in this resin as minor compounds. Therefore, the study suggests that *Jatobá* resin can be satisfactorily distinguished from other *Leguminosae* resins and from resins from other species of the same genus characterized in previous studies.

Analysis by THM–GC–MS is made problematic by the appearance of a number of secondary pyrolysis products as a result of reactions such as hydrolysis, isomerization, dehydration and recombination of the original *epi*-labdanoids a consequence of the strong alkalinity of the TMAH solution. On-line trimethylsilylation Py–GC–MS and off-line methylation with MCF with MCF on the other hand were unable to derivatize iso-ozic and *epi*-pinifolic acid. The comparison of the results obtained from the three analytical methods applied has enabled a satisfactory discrimination between the original compounds present in the resin specimens and those others yielded as a result of secondary reactions taking place during the pyrolysis process.

The absence of pyrolysis products of the polymeric fraction in the samples from unaged and UV light-aged thin film specimens evidences the low tendency of *Jatobá* resin to polymerize, which coincides with the absence of *epi*-labdanoids of the ozic series found in the samples analyzed, and also with the high solubility in polar solvents exhibited by the unaged resin and by the unaged and UV light-aged films.

The main changes in composition found after UV light ageing of the thin film specimens include the appearance of a new isomer of eperuic acid. The formation of unidentified oxidized compounds bearing hydroxyl or ketone groups has been supported by the IR absorption spectra of the aged thin films. Changes in the relative content of the major compounds present in the unaged and aged thin film specimens have been observed, which require further study in order to understand the effect of the different environmental agents acting during atmospheric exposure of the thin films and UV light ageing.

Acknowledgements

Financial support is gratefully acknowledged from the Spanish "I+D+I MEC" project CTQ2005-09339-CO3-01 and CTQ2008-06727-C03-01/BQU which are also supported by FEDER funds and the Generalitat Valenciana "I+D+I" project ACOMP/2007/138.

References

[1] A. Cunningham, S.S. Martin, J.H. Langenheim, Phytochemistry 12 (1973) 633.
[2] Y.T. Lee, J.H. Langenheim, Systematics of The Genus *Hymenaea* L. (Leguminosae, Caesalpinoideae, Detarieae), vol. 69, Chemistry of California Press Ltd., 1975, p. 1.
[3] J.H. Langenheim, Y.T. Lee, S.S. Martin, Am. J. Bot. 57 (1970) 754.
[4] J.H. Langenheim, Y.T. Lee, S.S. Martin, Am. J. Bot. 58 (1971) 466.
[5] J.H. Langenheim, Plant Resins: Chemistry, Evolution, Ecology and Ethnobotany, Timber Press, Portland, Cambridge, 2003.
[6] A. Cunningham, S.S. Martin, J.H. Langenheim, Phytochemistry 13 (1974) 294.
[7] A.J. Marsaioli, H. de Freitas Leitao Jr., J. de Paiva Campello, Phytochem. Rep. 14 (1975) 1882.
[8] R.T. Nogueira, G.J. Sheperd, A. Laverde Jr., A.J. Marsaioli, P.M. Imamura, Phytochemistry 58 (2001) 1153.
[9] S.F. Khoo, A.C. Ochlschlager, G. Ourisson, Tetrahedron 29 (1973) 3379.
[10] T. Nakano, C. Djerassi, J. Org. Chem. 26 (1961) 167.
[11] S.S. Martin, J.H. Langenheim, Phytochemistry 13 (1974) 523.
[12] G.O. Poinar Jr., Experientia 47 (1991) 1075.
[13] H.C. Bryson, Paint Manuf. 22 (1952) 243.
[14] R.J. Gettens, G.L. Stout, Painting Materials a Short Encyclopaedia, Dover Publications, New York, 1966.
[15] J.P. Echard, C. Benoit, J. Peris-Vicente, V. Malecki, J.V. Gimeno-Adelantado, S. Vaiedelich, Anal. Chim. Acta 584 (2007) 172.
[16] G.D. Hiscox, A.A. Hopkins, Henley's Twentieth Century Formulas, Recipes and Processes. The Scientific American Cyclopedia of Formulas, second Spanish ed., G. Gili, Mexico, 1997, p. 953.
[17] J. de la Cruz-Cañizares, M.T. Doménech-Carbó, R. Mateo-Castro, J.V. Gimeno-Adelantado, F. Bosch-Reig, J. Chromatogr. A 1093 (2005) 177.
[18] L.A.C. Souza, C. Avila, Painted Wood: History and Conservation. Historical Materials and Technique, The Getty Conservation Institute, Los Angeles, 1998, p. 206.
[19] J.S. Mills, R. White, Stud. Conserv. 22 (1977) 12.
[20] L. Masschelein-Kleiner, P. Taets, 6th triennial meeting of the ICOM Committee for Conservation, Ottawa, 1981, 81/16/3.
[21] M.P. Colombini, F. Modugno, S. Giannarelli, R. Fuoco, M. Matteini, Microchem. J. 67 (2000) 385.
[22] L. Osete-Cortina, M.T. Doménech-Carbó, J.V. Gimeno-Adelantado, R. Mateo-Castro, F. Bosch-Reig, J. Chromatogr. A 1024 (2004) 187.
[23] B. Singer, R. McGuigan, Ann. Chim. 97 (2007) 405.
[24] R. Stevanato, M. Rovea, M. Carbini, D. Favretto, P. Traldi, Rapid Commun. Mass Spectrom. 11 (1997) 286.
[25] K.J. van den Berg, J.J. Boon, I. Pastorova, L.F.M. Spetter, J. Mass Spectrom. 35 (2000) 512.
[26] D. Scalarone, M. Lazzari, O. Chiantore, J. Anal. Appl. Pyrolysis 68–69 (2003) 115.
[27] I.D. van der Werf, K.J. van den Berg, S. Schmitt, J.J. Boon, Stud. Conserv. 45 (2000) 1.
[28] K.J. Van den Berg, I. Pastorova, L. Spetter, J.J. Boon, Preprints of the 10th Triennial Meeting ICOM Committee for Conservation, Edinburgh, 1996, p. 930.
[29] D. Scalarone, M. Lazzari, O. Chiantore, J. Anal. Appl. Pyrolysis 64 (2002) 345.
[30] M.P. Colombini, I. Bonaduce, F. Modugno, Chromatographia 58 (2003) 357.
[31] G. Chiavari, D. Fabbri, S. Prati, Chromatographia 55 (2002) 611.
[32] L. Osete-Cortina, M.T. Doménech-Carbó, J. Chromatogr. A 1065 (2005) 265.
[33] K.J. van den Berg, J. van der Horst, J.J. Boon, Preprints of the ICOM-CC 12th Triennial Meeting, Lyon, 1999, p. 855.
[34] K.J. van den Berg, J.J. Ossebaar, H. van Keulen, in: R. van Grieken, K. Janssens, L. Van'tdack, G. Meersman (Eds.), Preprints of Art 2002: Seventh International Conference on Non-Destructive Testing and Microanalysis for Diagnostics and Conservation of the Cultural and Environmental Heritage, Antwerp, 2002, University of Antwerp, Antwerp, 2002, p. 10.
[35] J.S. Mills, R. White, The Organic Chemistry of Museum Objects, Butterworths, London, 1987.
[36] K.B. Anderson, R.E. Winans, Anal. Chem. 63 (1991) 2901.
[37] K.B. Anderson, Geochem. Trans. 3 (2001) 21.
[38] K.B. Anderson, Org. Geochem. 2 (1994) 209.
[39] P. Sargent Bray, K.B. Anderson, Geochem. Trans. 9 (2008) 3.
[40] K.B. Anderson, Geochem. Trans. 7 (2006) 2.
[41] K.B. Anderson, W. Bray, Archaeometry 48 (2006) 633.
[42] J.H. Langenheim, Science 163 (1969) 1157.
[43] C.P. Jácome, Ayquatiá da Yapepó. Estudo dos Materiais Utilizados na Cerâmica Pintada Tupiguarani de Minas Gerais, Dissertaçao de Mestrado em Artes Visuais da Escola de Belas Artes da Universidade Federal de minas Gerais, 2006.
[44] H. Lorenzi, Arvores Brasileiras, vol. 1, fourth ed., Plantarum, Sao Paulo, 2002.
[45] G. Hugel, G. Ourisson, Bull. Soc. Chim. (1965) 2903.
[46] C.R. Enzell, R. Ryhage, Arkiv für Kemi. 23 (1964) 367.
[47] C. Enzell, Acta Chem. Scand. 15 (1961) 1303.
[48] K. Biemann, Mass Spectrometry Organic Chemical Applications, McGraw-Hill, New York, 1962.
[49] C. Asselineau, S. Bory, M. Fetizon, P. Laszlo, Bull. Soc. Chim. France (1961) 1429.